

Influence of magnetic field on generalized piezo-thermoelastic rotating medium with two relaxation times

Mohamed I. A. Othman^{1,2} · Yassmin D. Elmaklizi³ · Ethar A. A. Ahmed²

Received: 15 January 2017 / Accepted: 31 July 2017 / Published online: 7 August 2017
© Springer-Verlag GmbH Germany 2017

Abstract In the present paper, the two different theories (coupled theory and Green–Lindsay theory with two relaxation times) are applied to study the deformation of a generalized piezo-thermoelastic rotating medium under the influence of magnetic field. The normal mode analysis is used to obtain the expressions for the displacement components, the temperature, the stress, the strain components, the electric potential and the electric displacements. Numerical results for the field quantities are given in the physical domain and illustrated graphically. Comparisons are made with the results predicted by coupled and Green–Lindsay theories in the presence and absence of rotation as well as magnetic field.

List of symbols

u_i	Mechanical displacement
T	Absolute temperature
σ_{ij}	Stress tensor
E_i	Electric field
C_{ijkl}	Elastic parameters tensor

ϵ_{ij}	Dielectric moduli
\mathbf{J}	Current density vector
\mathbf{E}	Induced electric field vector
K_{ij}	Heat conduction tensor
C_e	Specific heat at constant strain
α_1, α_3	Coefficients of linear thermal expansion
ϵ_0, μ_0	Electric and magnetic permeability respectively
$v_p = \sqrt{\frac{C_{11}}{\rho}}$	Longitudinal wave velocity in the medium
φ	Electric potential
ϵ_{ij}	Strain tensor
β_{ij}	Thermal elastic coupling tensor
D_i	Electric displacement
e_{kij}	Piezoelectric moduli
p_i	Pyroelectric moduli
\mathbf{h}	Induced magnetic field vector
ρ	Mass density
T_0	Reference temperature
t_0, t_1	Thermal relaxation time parameters

✉ Mohamed I. A. Othman
m_i_a_othman@yahoo.com

Yassmin D. Elmaklizi
jass.dess@gmail.com

Ethar A. A. Ahmed
ethar_ahmed54@yahoo.com

¹ Department of Mathematics, Faculty of Science, Taif University, 888, Taif, Saudi Arabia

² Department of Mathematics, Faculty of Science, Zagazig University, P.O. Box 44519, Zagazig, Egypt

³ Department of Mathematics, Faculty of Science, Suez Canal University, Ismailia, Egypt

1 Introduction

The brothers Curie and Curie (1880) was discovered the piezoelectricity when electric charges were created by mechanical stress on the surface of tourmaline crystals. The first application of piezoelectric materials was used as resonators for ultrasound sources in sonar devices. The better type's piezoelectric materials such as Barium Titanate are obtained by the development of the materials. Recently, breakthrough in single crystal growth technique has led to the development of high strain and high electric breakdown piezoceramics by Tichy et al. (2010). Mindlin (1961) discussed first the theory of thermo-piezoelectricity.

Nowachi (1978, 1983) investigated the physical laws for the thermo-piezo-electric materials. Chandrasekharaiah (1984, 1988) studied the generalized linear thermoelasticity theory for piezoelectric media. He et al. (2002a, b) investigated two dimensional generalized thermal shock problem of a thick piezo-electric plate of infinite extent. They deduced that the generalized thermoelasticity theory, heat propagated as a wave with finite velocity. The propagation of Rayleigh waves in transversely isotropic piezo-thermoelastic materials are investigated by Sharma et al. (2005).

Youssef and Bassiouny (2008) discussed the two temperature generalized thermo-piezoelasticity for one dimensional problem with the state-space approach. They solved the governing equations in the Laplace transform domain by using the state-space approach of the modern control theory. Othman and Ahmed (2016) studied the influence of the gravitational field on piezo-thermoelastic rotating medium with G–L theory. Qin and Yang (2008) suggested the effective properties of thermo-piezoelectricity. Said (2016) studied the influence of gravity on generalized magneto-thermoelastic medium for three-phase-lag model. Othman and Kumar (2009) and Othman (2005) suggested the generalized electro-magneto-thermoelastic wave under different theories. El-Naggar and Abd-Alla (1989) studied Rayleigh waves in magneto-thermoelastic half-space under initial stress. Othman and Abbas (2014) studied the effect of rotation on plane waves in generalized thermo-microstretch elastic solid comparison of different theories using finite element method. Sharma and Kumar (2000) investigated the plane harmonic waves in piezo-thermoelastic materials. Schoenberg and Censor (1973) studied elastic waves in rotating media. Othman and Elmaklizi (2013) studied the 2-D problem of generalized magneto-thermoelastic diffusion with the temperature dependent elastic medium. Othman (2002) investigated Lord–Shulman theory under the dependence of the modulus of elasticity on the reference temperature in two-dimensional generalized thermoelasticity. Othman et al. (2014) studied the effect of rotation on micropolar generalized thermoelasticity with two-temperature using a dual-phase-lag model. Othman et al. (2013) studied the influence of the gravity field and rotation on a generalized thermoelastic medium using a dual-phase-lag model. Othman and Abbas (2015) used the finite element method to study the effect of rotation on a magneto-thermoelastic hollow cylinder with energy dissipation using.

Piezo-thermoelastic materials take into account the coupling effect of elastic, thermal and electric fields simultaneously. These materials can be used as sensors and actuators in smart structural systems undergoing thermo-mechanical excitation. The usefulness of piezoelectric

devices in such systems stems from the coupling that exists between the thermoelastic and electric fields. In sensor applications, thermomechanical disturbances can be determined from measurements of the induced electric potential differences (direct piezoelectric effect); in actuator applications, deformation and/or stress are controlled through the introduction of an appropriate electric field (converse piezo effect) (Ashida et al. 1994). Sensors made of these materials can be used in automatic fire control systems. In regards to aerospace applications, these structures are generally light and flexible enough to induce large deformation. In living bodies' bones, cartilage, tendons, ligaments, and nerve tissues are pyroelectric substances. PVF2 polymer is used in hydrophones that are used at great ocean depth. Piezo-thermo-elastic or thermo-piezoelectric sensors are also used in automatic fire control system.

The present work deals with the effect of rotation and magnetic field in a generalized piezo-thermoelastic. The normal mode analysis is used to obtain the exact expressions for the considered variables. The distributions of the considered variables are presented graphically. Numerical results for the field quantities are given and illustrated graphically in the presence and absence of the magnetic field and rotation.

2 Formulation of the problem

2.1 Basic equations

The basic governing field equations of generalized hexagonal piezo-thermoelastic for two-dimensional motion in x – z plane are (2000)

2.2 Strain–displacement-relation

$$\varepsilon_{ij} = \frac{1}{2}(u_{i,j} + u_{j,i}) \quad (1)$$

– Stress–strain-temperature:

$$\sigma_{ij} = C_{ijkl}\varepsilon_{kl} - e_{kij}E_k - \beta_{ij}\left(1 + t_1\frac{\partial}{\partial t}\right)T\delta_{ij}, \quad (2)$$

where $i, j, k, l = 1, 2, 3$.

2.3 Gauss equation and electric field relation

$$D_{i,i} = 0, \quad (3)$$

$$D_i = e_{ijk}\varepsilon_{jk} + \epsilon_{ij}E_j + p_i\left(1 + t_1\frac{\partial}{\partial t}\right)T, \quad (4)$$

where $E_i = -\varphi_{,i}$.

2.4 Heat conduction equation

$$K_{ij}T_{,ij} = \rho C_e \left(1 + t_0 \frac{\partial}{\partial t}\right) \dot{T} + T_0[\beta_{ij} \dot{u}_{i,j} - p_i \dot{\phi}_{,i}]. \tag{5}$$

2.5 Equation of motion

Since the medium is rotating uniformly with an angular velocity $\Omega = \Omega \mathbf{n}$ where \mathbf{n} is a unit vector representing the direction of the axis of the rotation, the equation of motion in the rotating frame of reference has two additional terms (Schoenberg and Censor 1973): centripetal acceleration $\Omega \wedge (\Omega \wedge \mathbf{u})$ due to time-varying motion only and Corioli’s acceleration $2\Omega \wedge \dot{\mathbf{u}}$, then the equation of motion in a rotating frame of reference and with body force is

$$\rho[\ddot{u}_i + \{\Omega \wedge (\Omega \wedge \mathbf{u})\}_i + (2\Omega \wedge \dot{\mathbf{u}})_i] = \sigma_{ij,j} + F_i, \tag{6}$$

where F_i is the Lorentz force and is given by:

$$F_i = \mu_0 (\mathbf{J} \times \mathbf{H})_i. \tag{7}$$

The variation of the magnetic and electric fields are perfectly conducting slowly moving medium and are given by Maxwell’s equations:

$$\text{curl } \mathbf{h} = \mathbf{J} + \varepsilon_0 \dot{\mathbf{E}}, \tag{8}$$

$$\text{curl } \mathbf{E} = -\mu_0 \dot{\mathbf{h}}, \tag{9}$$

$$\mathbf{E} = -\mu_0 (\dot{\mathbf{u}} \times \mathbf{H}), \tag{10}$$

$$\text{div } \mathbf{h} = 0. \tag{11}$$

Expressing components of the vector $\mathbf{J} = (J_1, J_2, J_3)$ in terms of the displacement by eliminating the quantities \mathbf{h} and \mathbf{E} from Eq. (8), thus yields

$$J_1 = -h_{,z} + \varepsilon_0 \mu_0 H_0 \ddot{w}, \quad J_2 = 0, \quad J_3 = h_{,x} + \varepsilon_0 \mu_0 H_0 \ddot{u}. \tag{12}$$

From Eqs. (8)–(11), it can be concluded that:

$$h = -H_0 e. \tag{13}$$

Substituting from Eq. (12) in Eq. (7), one can get

$$\mathbf{F} = (F_x, F_y, F_z) \\ = (\mu_0 H_0^2 e_{,x} - \varepsilon_0 \mu_0^2 H_0^2 \ddot{u}, 0, \mu_0 H_0^2 e_{,z} - \varepsilon_0 \mu_0^2 H_0^2 \ddot{w}). \tag{14}$$

The constitutive relation and electric displacement of the hexagonal (6 mm) crystal symmetry are given by

$$\sigma_{xx} = C_{11} \varepsilon_{xx} + C_{13} \varepsilon_{zz} - e_{31} E_z - \beta_1 \left(1 + t_1 \frac{\partial}{\partial t}\right) T, \tag{15}$$

$$\sigma_{zz} = C_{13} \varepsilon_{xx} + C_{33} \varepsilon_{zz} - e_{33} E_z - \beta_3 \left(1 + t_1 \frac{\partial}{\partial t}\right) T, \tag{16}$$

$$\sigma_{xz} = 2 C_{44} \varepsilon_{zx} - e_{15} E_x, \tag{17}$$

$$D_x = e_{15}(u_{,z} + w_{,x}) + \varepsilon_{11} E_x, \tag{18}$$

$$D_z = e_{31} u_{,x} + e_{33} w_{,z} + \varepsilon_{33} E_z + p_3 \left(1 + t_1 \frac{\partial}{\partial t}\right) T. \tag{19}$$

3 The boundary conditions:

1. A mechanical boundary condition

$$\sigma_{zz}(x, 0, t) = -f_1(x, 0, t) = -f_1^* \exp(ia(x - ct)), \\ \sigma_{xz}(x, 0, t) = 0, \quad \frac{\partial \varphi}{\partial z} = 0. \tag{20}$$

2. A thermal boundary condition that the surface of the half-space subjected to thermal shock

$$T(x, 0, t) = f_2(x, 0, t) = f_2^* \exp(ia(x - ct)), \tag{21}$$

where $f_1(x, t)$ and $f_2(x, t)$ are arbitrary functions of x, t and f_1^*, f_2^* are constant.

We consider a homogeneous, anisotropic, piezo-thermoelastic half-space of hexagonal type. The basic governing Eqs. (3)–(6) for the temperature change $T(x, z, t)$, displacement vector $\mathbf{u}(x, z, t) = (u, 0, w)$, and electric potential $\varphi(x, z, t)$, under the effect of rotation and magnetic field are given by,

$$C_{11} u_{,xx} + C_{44} u_{,zz} + (C_{13} + C_{44}) w_{,xz} + (e_{31} + e_{15}) \varphi_{,xz} \\ - \beta_1 \left(1 + t_1 \frac{\partial}{\partial t}\right) T_{,x} + \mu_0 H_0^2 e_{,x} \\ - \varepsilon_0 \mu_0^2 H_0^2 \ddot{u} = \rho (\ddot{u} - \Omega^2 u + 2\Omega \dot{w}), \tag{22}$$

$$(C_{44} + C_{13}) u_{,xz} + C_{44} w_{,xx} + C_{33} w_{,zz} + e_{15} \varphi_{,xx} \\ + e_{33} \varphi_{,zz} - \beta_3 \left(1 + t_1 \frac{\partial}{\partial t}\right) T_{,z} + \mu_0 H_0^2 e_{,z} \\ - \varepsilon_0 \mu_0^2 H_0^2 \ddot{w} = \rho (\ddot{w} - \Omega^2 w - 2\Omega \dot{u}), \tag{23}$$

$$(e_{15} + e_{31}) u_{,xz} + e_{15} w_{,xx} + e_{33} w_{,zz} - \varepsilon_{11} \varphi_{,xx} \\ - \varepsilon_{33} \varphi_{,zz} + p_3 \left(1 + t_1 \frac{\partial}{\partial t}\right) T_{,z} = 0, \tag{24}$$

$$K_1 T_{,xx} + K_3 T_{,zz} - \rho C_e \left(1 + t_0 \frac{\partial}{\partial t}\right) \dot{T} \\ = T_0 [\beta_1 \dot{u}_{,x} + \beta_3 \dot{w}_{,z} - p_3 \dot{\phi}_{,z}]. \tag{25}$$

To facilitate the solution, the following non-dimensional quantities are introduced

$$x' = \frac{\omega^*}{v_p} x, \quad z' = \frac{\omega^*}{v_p} z, \quad u' = \frac{\rho \omega^* v_p}{\beta_1 T_0} u, \quad w' = \frac{\rho \omega^* v_p}{\beta_1 T_0} w, \\ T' = \frac{T}{T_0}, \quad \sigma'_{ij} = \frac{\sigma_{ij}}{\beta_1 T_0}, \quad \varphi' = \varepsilon_p \varphi,$$

$$\{t', t'_1, t'_0\} = \omega^* \{t, t_1, t_0\}, \quad D'_i = \frac{D_i}{e}, \quad \Omega' = \frac{\Omega}{\omega^*}, \quad (26)$$

where $\omega^* = \frac{C_e C_{11}}{K_{11}}$, $\varepsilon_p = \frac{\omega^* \varepsilon_{33}}{\nu_p \beta_1 T_0}$, $\beta_1 = (C_{11} + C_{12}) \alpha_1 + C_{13} \alpha_3$, $\beta_3 = 2C_{13} \alpha_1 + C_{33} \alpha_3$.

In terms of the non-dimensional quantities defined in Eq. (26), the above governing Eqs. (22)–(25) take the form (dropping the primes over the non-dimensional variables for convenience)

$$\delta_1 u_{,xx} + \delta_2 u_{,zz} + \delta_3 w_{,xz} + \delta_4 \varphi_{,xz} - \left(1 + t_1 \frac{\partial}{\partial t}\right) T_{,x} = \delta_5 \ddot{u} - \Omega^2 u + 2\Omega \dot{w}, \quad (27)$$

$$\delta_3 u_{,xz} + \delta_2 w_{,xx} + \delta_6 w_{,zz} + \delta_7 \varphi_{,xx} + \varphi_{,zz} + \delta_8 \left(1 + t_1 \frac{\partial}{\partial t}\right) T_{,z} = \delta_5 \ddot{w} - \Omega^2 w - 2\Omega \dot{u}, \quad (28)$$

$$\delta_9 u_{,xz} + \delta_{10} w_{,xx} + \delta_{11} w_{,zz} + \delta_{12} \varphi_{,xx} + \delta_{13} \varphi_{,zz} + \delta_{14} \left(1 + t_1 \frac{\partial}{\partial t}\right) T_{,z} = 0, \quad (29)$$

$$\delta_{15} T_{,xx} + \delta_{16} T_{,zz} - \left(1 + t_0 \frac{\partial}{\partial t}\right) \dot{T} = [\delta_{17} \dot{u}_{,x} + \delta_{18} \dot{w}_{,z} + \delta_{19} \dot{\varphi}_{,z}], \quad (30)$$

where δ_j , $j = 1 - 19$ are given in “Appendix A”.

4 The solution of the problem

In this section, we applied the normal mode analysis, which gives exact solutions without any assumed restrictions on the displacement, stress distributions and temperature. It is applied to a wide range of problems in different branches (Othman (2002) and Othman et al. (2013, 2014, 2015)).

The solution of the considered physical quantities can be decomposed in terms of the normal mode in the following form:

$$[u, w, \varphi, T](x, z, t) = [u^*, w^*, \varphi^*, T^*](z) \exp(ia(x - ct)). \quad (31)$$

where $D = \frac{d}{dz}$, $c = \frac{\omega}{a}$, ω is the complex time constant (frequency), i is the imaginary unit, a is the wave number in the x direction, u^* , w^* , φ^* and T^* are the amplitudes of the functions u , w , φ , T .

Substituting from Eq. (31) in Eqs. (27)–(30), we get

$$(D^2 + A_1) u^* + (A_2 D + A_3) w^* + A_4 D \varphi^* + A_5 T^* = 0, \quad (32)$$

$$(A_6 D + A_7) u^* + (D^2 + A_8) w^* + (A_9 D^2 + A_{10}) \varphi^* + A_{11} D T^* = 0, \quad (33)$$

$$A_{12} D u^* + (D^2 + A_{13}) w^* + (A_{14} D^2 + A_{15}) \varphi^* + A_{16} D T^* = 0, \quad (34)$$

$$A_{17} u^* + A_{18} D w^* + A_{19} D \varphi^* + (D^2 + A_{20}) T^* = 0, \quad (35)$$

where A_j , $j = 1 - 20$ are given in “Appendix A”.

Equations (32)–(35) have a non-trivial solution if the determinant coefficients of the physical quantities equal to zero, then we get

$$[D^8 - A D^6 + B D^4 - C D^2 + E] \{u^*(z), w^*(z), \varphi^*(z), T^*(z)\} = 0, \quad (36)$$

where A , B , C , E are given in “Appendix A”.

Equation (36) can be factored as

$$(D^2 - k_1^2)(D^2 - k_2^2)(D^2 - k_3^2)(D^2 - k_4^2) \{u^*(z), w^*(z), \varphi^*(z), T^*(z)\} = 0. \quad (37)$$

The solution of Eq. (37), bound as $z \rightarrow \infty$, is given by

$$u^* = \sum_{n=1}^4 M_n \exp(-k_n z), \quad (38)$$

$$w^* = \sum_{n=1}^4 H_{1n} M_n \exp(-k_n z), \quad (39)$$

$$\varphi^* = \sum_{n=1}^4 H_{2n} M_n \exp(-k_n z), \quad (40)$$

$$T^* = \sum_{n=1}^4 H_{3n} M_n \exp(-k_n z), \quad (41)$$

where k_n^2 ($n = 1, 2, 3, 4$) are the roots of the characteristic equation of Eq. (37).

By taking a non-dimension and the normal mode to Eqs. (15)–(19) then substituting from Eqs. (38)–(41), we obtain

$$\sigma_{xx}^* = \sum_{n=1}^4 H_{4n} M_n \exp(-k_n z), \quad (42)$$

$$\sigma_{zz}^* = \sum_{n=1}^4 H_{5n} M_n \exp(-k_n z), \quad (43)$$

$$\sigma_{xz}^* = \sum_{n=1}^4 H_{6n} M_n \exp(-k_n z), \quad (44)$$

$$D_x^* = \sum_{n=1}^4 H_{7n} M_n \exp(-k_n z), \quad (45)$$

$$D_z^* = \sum_{n=1}^4 H_{8n} M_n \exp(-k_n z), \quad (46)$$

where H_{jn} , $j = 1 - 8$, $n = 1, 2, 3, 4$ are given in “Appendix B”.

By applying the boundary conditions (20) and (21) to determine $M_n(n = 1, 2, 3, 4)$, we obtain

$$\sum_{n=1}^4 H_{5n}M_n = -f_1^* \tag{47}$$

$$\sum_{n=1}^4 H_{6n}M_n = 0, \tag{48}$$

$$\sum_{n=1}^4 k_n H_{2n}M_n = 0, \tag{49}$$

$$\sum_{n=1}^4 H_{3n}M_n = f_2^*. \tag{50}$$

By solving the above system of Eqs. (47)–(50), of $M_n(n = 1, 2, 3, 4)$ by using the inverse of matrix method as follows:

$$\begin{pmatrix} M_1 \\ M_2 \\ M_3 \\ M_4 \end{pmatrix} = \begin{pmatrix} H_{51} & H_{52} & H_{53} & H_{54} \\ H_{61} & H_{62} & H_{63} & H_{64} \\ k_1 H_{21} & k_2 H_{22} & k_3 H_{23} & k_4 H_{24} \\ H_{31} & H_{32} & H_{33} & H_{34} \end{pmatrix}^{-1} \begin{pmatrix} -f_1^* \\ 0 \\ 0 \\ f_2^* \end{pmatrix}. \tag{51}$$

5 Numerical results and discussions

For study the effect of rotation and magnetic field, we will apply the numerical results. The material chosen for the purpose of numerical calculations is taken as Cadmium Selenide (CdSe) having hexagonal symmetry (6 mm class)

$C_{11} = 7.41 \times 10^{10} \text{ Nm}^{-2}$, $C_{12} = 4.52 \times 10^{10} \text{ Nm}^{-2}$,
 $C_{13} = 3.93 \times 10^{10} \text{ Nm}^{-2}$, $C_{33} = 8.36 \times 10^{10} \text{ Nm}^{-2}$,
 $C_{44} = 1.32 \times 10^{10} \text{ Nm}^{-2}$, $T_0 = 298 \text{ K}$, $\rho = 5504 \text{ Kg m}^{-3}$,
 $e_{13} = -0.160 \text{ Cm}^{-2}$, $e_{33} = 0.347 \text{ Cm}^{-2}$, $e_{15} = -0.138 \text{ Cm}^{-2}$,
 $\beta_1 = 0.621 \times 10^6 \text{ Nk}^{-1} \text{ m}^{-2}$, $\beta_3 = 0.551 \times 10^6 \text{ NK}^{-1} \text{ m}^{-2}$,
 $p_3 = -2.94 \times 10^{-6} \text{ CK}^{-1} \text{ m}^{-2}$, $K_1 = K_3 = 9 \text{ Wm}^{-1} \text{ K}^{-1}$,
 $\epsilon_{11} = 8.26 \times 10^{-11} \text{ C}^2 \text{ N}^{-1} \text{ m}^{-2}$, $\epsilon_{33} = 9.03 \times 10^{-11} \text{ C}^2 \text{ N}^{-1} \text{ m}^{-2}$,
 $C_e = 260 \text{ J Kg}^{-1} \text{ K}^{-1}$. The numerical technique, outlined above, was used for the distribution of the real part of the displacement component u , the temperature T , the stress components σ_{zz} , σ_{xz} the electric potential φ and the electric displacement D_z for the problem. Here, all variables are taken in non-dimensional form. The results are shown in Figs. 1, 2, 3, 4, 5, 6, 7, 8, 9, 10, 11 and 12; the graph shows four curves predicted by two theories of thermoelasticity. In these figures, the solid lines represent the solution in the coupled theory (CT) and the dashed lines represent the solution derived using (G–L) theory.

Figures 1, 2, 3, 4, 5 and 6 show the comparisons between the considered variables in the absence and presence of rotation (i.e. $\Omega = 0, 0.5$) at $H_0 = 10^8$. The computations are carried out for the non-dimensional time $t = 0.1$ on the surface plane $x = 1.5$, $f_1^* = 10$, $f_2^* = 10$.

Figure 1 depicts that the distribution of the horizontal displacement u , in the context the (CT) and (G–L) theories, always begins from negative values for $\Omega = 0, 0.5$. It shows that the values of u based on the (CT) and (G–L) theories increase then decrease and converges to zero for $\Omega = 0, 0.5$. Figure 2 demonstrates that the distribution of the temperature T . In the context of the (CT) and (G–L) theories and in the absence and presence of a rotation (i.e. $\Omega = 0, 0.5$), the distribution of T are increasing to the maximum value in the range $0 \leq z \leq 0.2$ then decreases and converges to zero. Figure 3 shows that the distribution of the stress components σ_{zz} , in the context of the (CT) theory the value of σ_{zz} decreases in the range $0 \leq z \leq 0.2$, then increases in the range $0.2 \leq z \leq 1.5$, for $\Omega = 0, 0.5$, while in the context of (G–L) theory, it is observed that the value of σ_{zz} decreases in the range $0 \leq z \leq 0.2$, then increase in the range $0.2 \leq z \leq 1$, then decrease and finally converges to zero for $\Omega = 0, 0.5$. Figure 4 clarifies that the distribution of the stress component σ_{xz} , in the context of the (CT) and (G–L) theories, begins from zero and satisfies the boundary conditions at $z = 0$. In the context of the two theories, the values of σ_{xz} decreases in the range $0 \leq z \leq 0.3$, then increases for $\Omega = 0, 0.5$. It is observed that the values of the stress components σ_{xz} at $\Omega = 0$ are higher than those at $\Omega = 0.5$. Figure 5 exhibits the distribution of the electric potential φ , in the context of the (CT) theory for $\Omega = 0, 0.5$, the values of φ decreases then increases and converges to zero. However, in the context of (G–L) theory the values of φ increases, then decrease for $\Omega = 0, 0.5$. It is observed that the values of the electric potential φ , in the context of the (G–L) for $\Omega = 0, 0.5$, are higher than the values of the electric potential φ , in the context of the (CT) for $\Omega = 0, 0.5$. Figure 6 depicts that the distribution of the electric displacement D_z , in the context the (CT) and (G–L) theories, always begins from positive values for $\Omega = 0, 0.5$. It shows that the values of D_z , based on the (CT) and (G–L) theories decrease then increase and finally converges to zero for $\Omega = 0, 0.5$.

Figures 7, 8, 9, 10, 11 and 12 show the comparisons between the considered variables in the absence and presence of a magnetic field (i.e. $H_0 = 0, 10^9$) at $\Omega = 0.5$.

Figure 7 shows that the distribution of the horizontal displacement u , in the context of (CT) and (G–L) theories, the value of u , increase in the range $0 \leq z \leq 0.5$, then decreases in the range $0.5 \leq z \leq 3$, for $H_0 = 0$. It is observed that in the case of absence of magnetic field the two curves of the (CT) and (G–L) theories are coincide,

Fig. 1 Horizontal displacement distribution u in the absence and presence of rotation

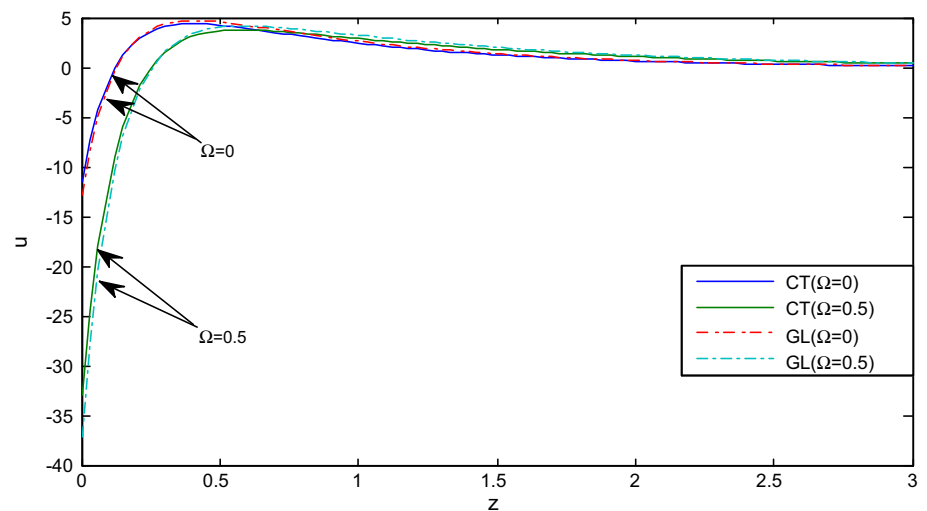


Fig. 2 Temperature distribution T in the absence and presence of rotation

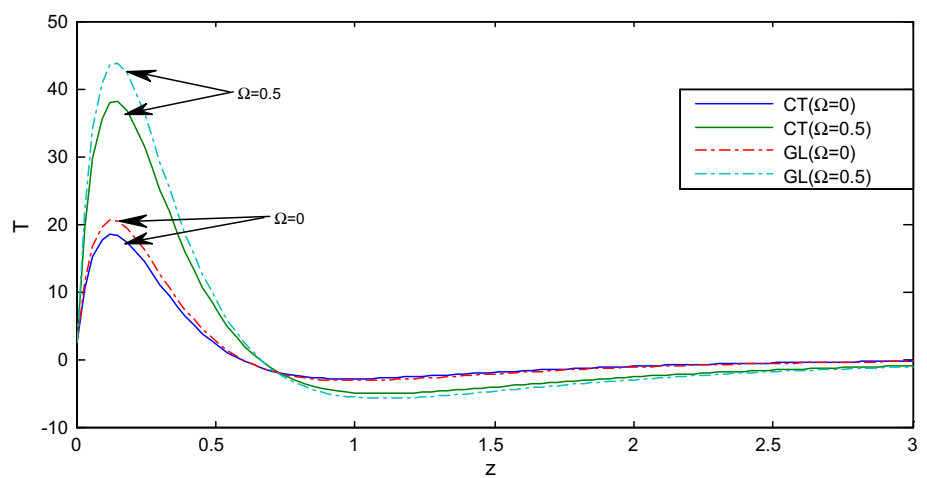
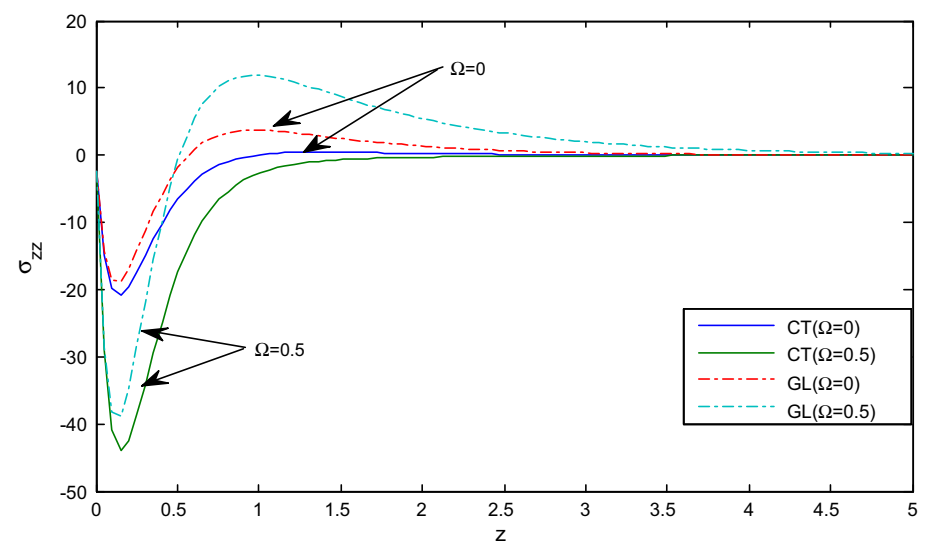


Fig. 3 Distribution of stress component σ_{zz} in the absence and presence of rotation



while for $H_0 = 10^9$, it is observed that the value of u , decreases then converges to zero. Figure 8 shows the distribution of temperature T . For $H_0 = 0$, the value of T

increase to the maximum value in the range $0 \leq z \leq 0.2$, then decrease in the range $0.2 \leq z \leq 1$, then increase in the range $1 \leq z \leq 3.5$, and finally converges to zero. For $H_0 =$

Fig. 4 Distribution of stress component σ_{xz} in the absence and presence of rotation

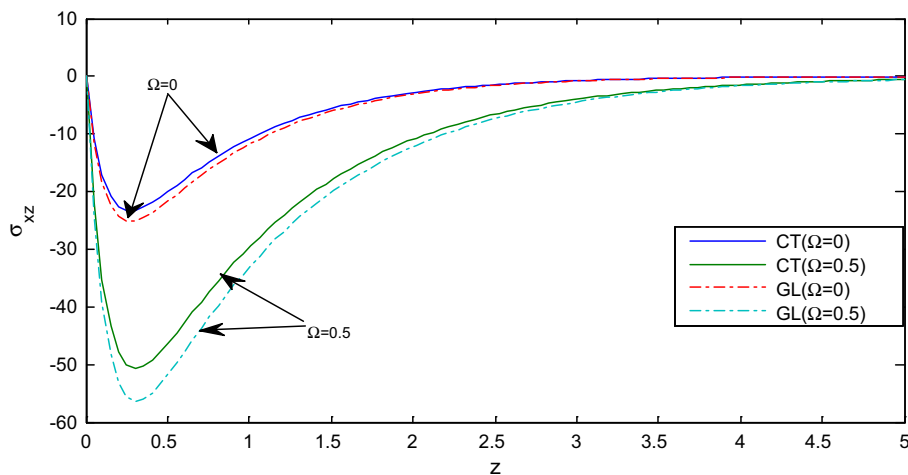


Fig. 5 Distribution of electric potential ϕ in the absence and presence of rotation

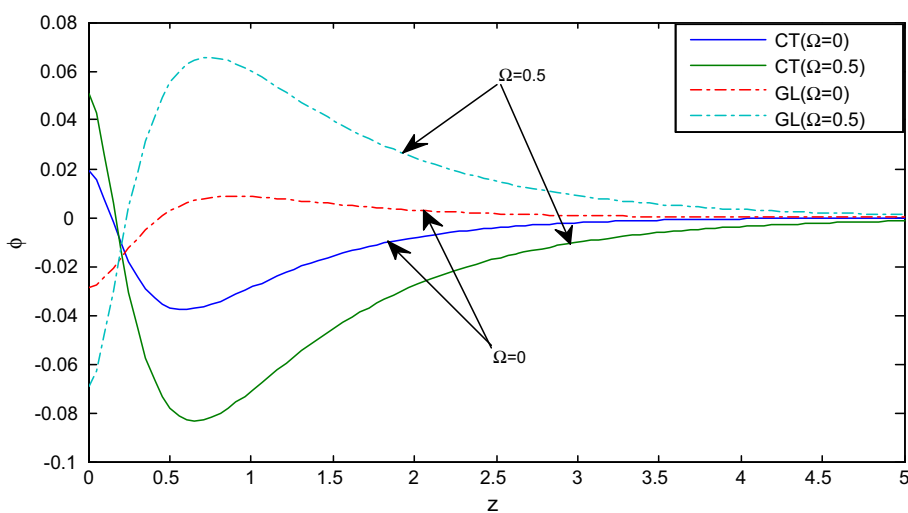
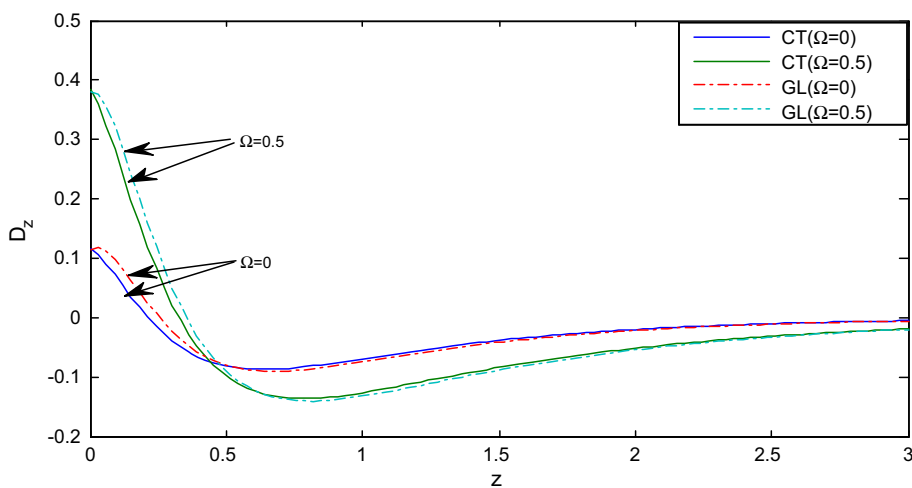


Fig. 6 Distribution of electric displacement component D_z in the absence and presence of rotation



10^9 , the value of T decreases, then increase and finally converge to zero in the context of the (CT) and (G–L) theories. Figure 9 represents the distribution of the stress

component σ_{zz} , in the context of the (CT) and (G–L) theories, always begins from negative values for $H_0 = 0, 10^9$. In the case of absence of the magnetic field the curve which

Fig. 7 Horizontal displacement distribution u in the absence and presence of magnetic field

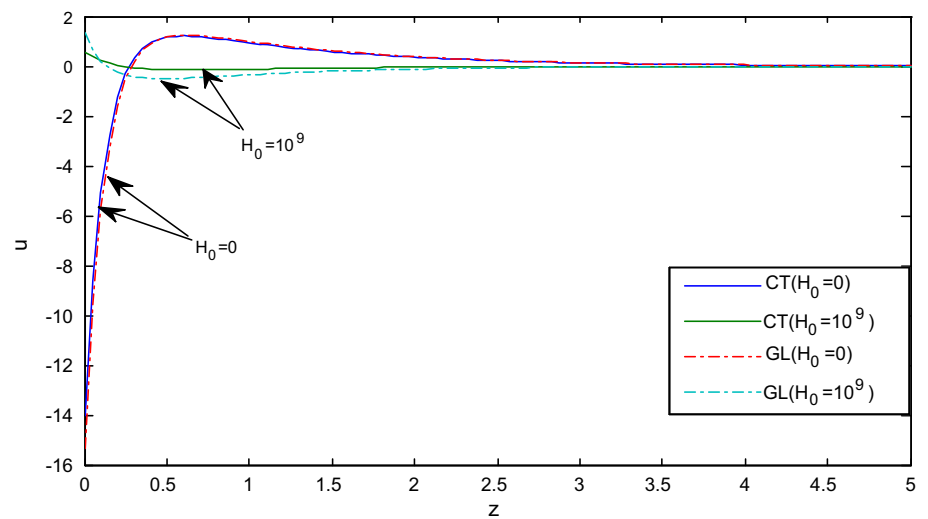


Fig. 8 Temperature distribution T in the absence and presence of magnetic field

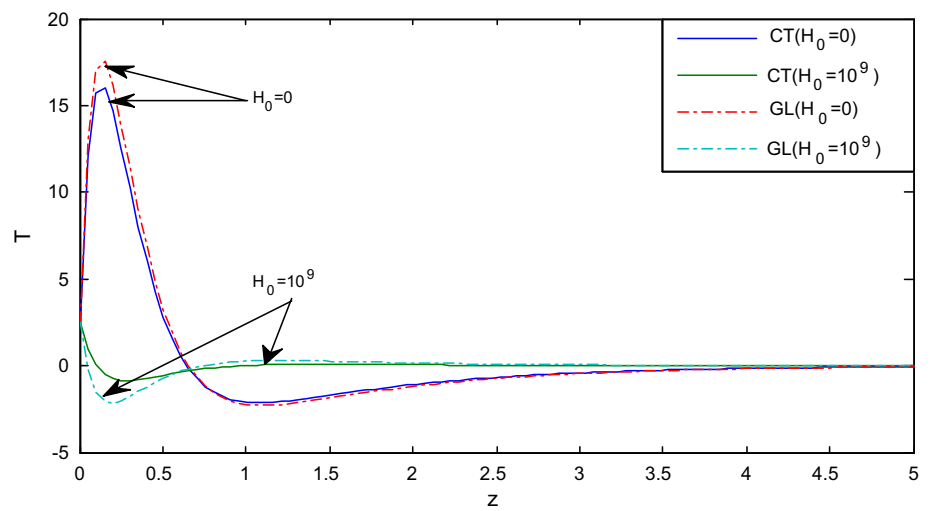
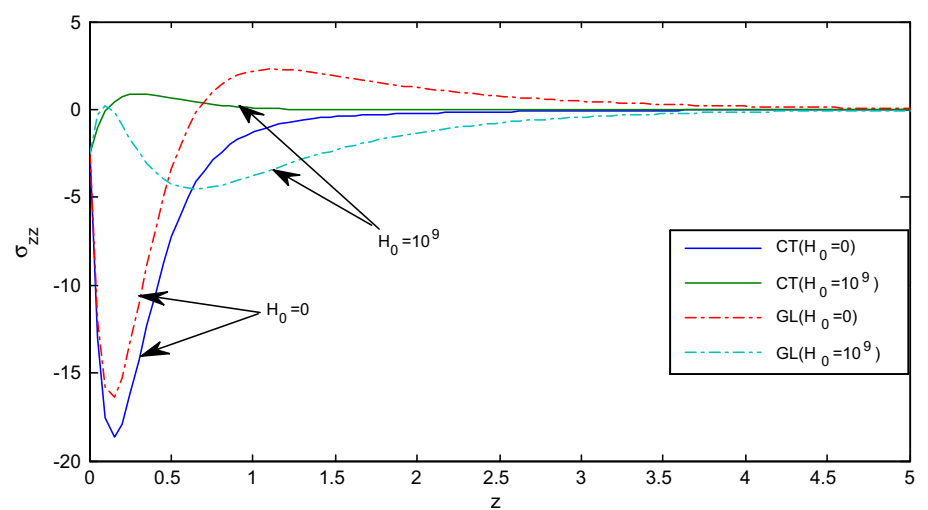


Fig. 9 Distribution of stress component σ_{zz} in the absence and presence of magnetic field



represent (CT) theory decreases to the minimum value in the range $0 \leq z \leq 0.2$, then increase and converge to zero at $z \geq 1.5$, while the curve which represent the (G–L) theory

decreases to the minimum value in the range $0 \leq z \leq 0.2$, then increases in the range $0.2 \leq z \leq 1$, then decrease and converge to zero at $z \geq 2.5$. However, in the case of the

Fig. 10 Distribution of stress component σ_{xz} in the absence and presence of magnetic field

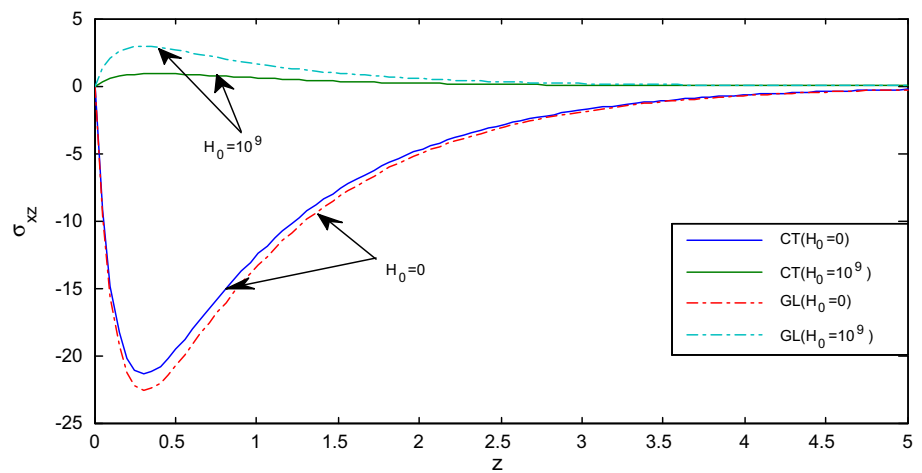


Fig. 11 Distribution of electric potential ϕ in the absence and presence of magnetic field

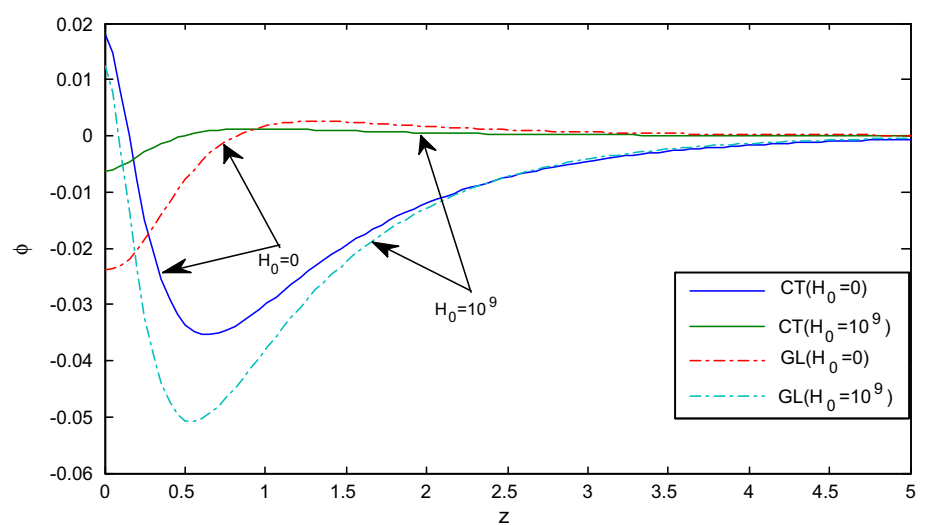
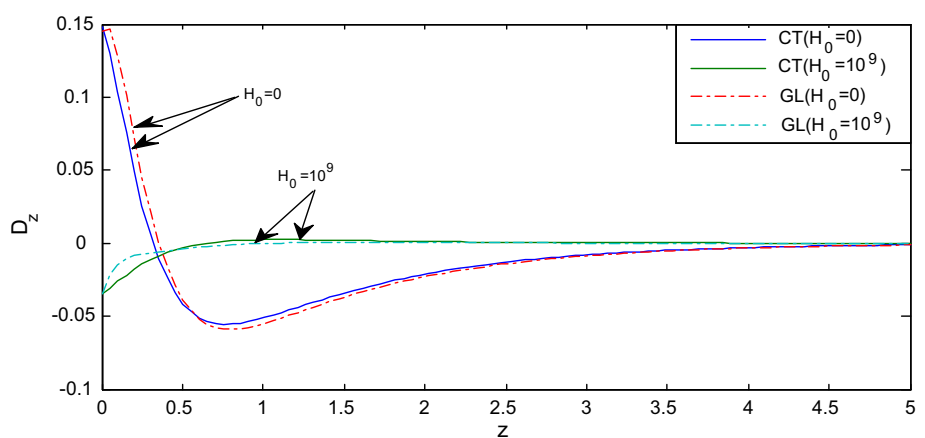


Fig. 12 Distribution of electric displacement component D_z in the absence and presence of magnetic field



presence of a magnetic field the curve, which represents (CT) theory has increased then decreased while the curve, which represent (G–L) theory is an increase in the range $0 \leq z \leq 0.1$, then decrease in the range $0.1 \leq z \leq 0.5$, then

increase and converge to zero at $z \geq 3.5$. Figure 10 exhibits that the distribution of the stress component σ_{xz} in the context of the (CT) and (G–L) theories, begins from zero and satisfies the boundary conditions at $z = 0$. In the

Fig. 13 (3D) Distribution of the displacement component u versus the components of distance based on (G–L) model at $\Omega = 0.5$ and $H_0 = 10^8$

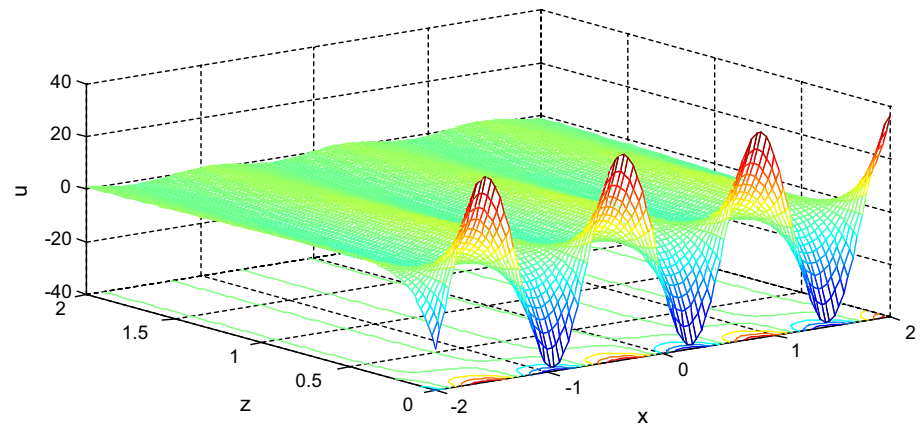
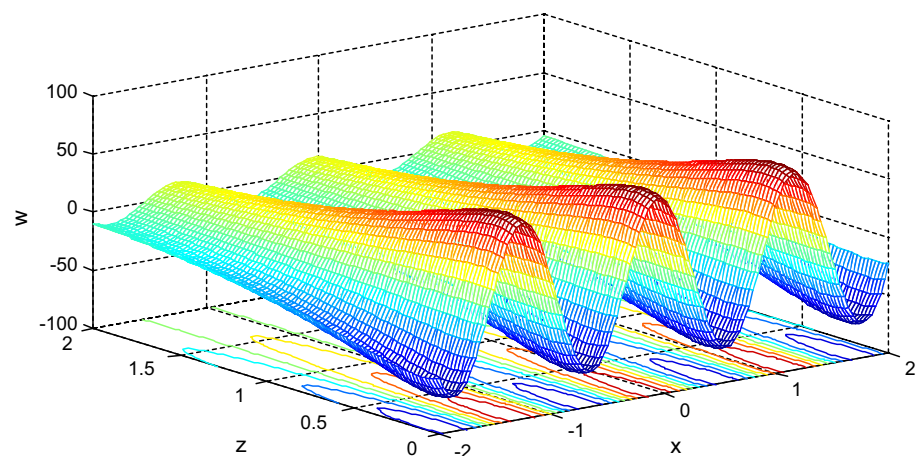


Fig. 14 (3D) Distribution of the displacement component w versus the components of distance based on (G–L) model at $\Omega = 0.5$ and $H_0 = 10^8$



context of the two theories, the values of σ_{xz} decreases in the range $0 \leq z \leq 0.3$, then increase for $H_0 = 10^9$. However, in the case of absence of the magnetic field the values of σ_{xz} increases then decreases and converges to zero. It is observed that the values of the stress components σ_{xz} at $H_0 = 10^9$, are higher than those at $H_0 = 0$. Figure 11 represents the variations of the electric potential φ , in the context of the (CT) and (G–L) theories, the values of φ , decreases in the range $0 \leq x \leq 0.5$, then increases for (CT) at $H_0 = 0$, and (G–L) at $H_0 = 10^9$, while in the case of (CT) at $H_0 = 10^9$, and (G–L) at $H_0 = 0$, it is observed that the value of φ , increases then decreases and converges to zero. Figure 12 shows that the distribution of the electric displacement D_z , in the context of (CT) and (G–L) theories, the value of D_z , decrease in the range $0 \leq x \leq 0.7$, then increases for $H_0 = 0$, while for $H_0 = 10^9$, it is observed that the value of D_z , increases then converges to zero.

3D curves Figs. 13, 14, 15, 16, 17 and 18 are representing the relation between the physical variables and both components of the distance, in the presence of rotation

$\Omega = 0.5$ and magnetic field $H_0 = 10^8$ in a generalized piezo-thermoelastic medium, in the context of (G–L). These figures are very important to study the dependence of these physical quantities on the vertical component of distance. The curves obtained are highly depending on the vertical distance and all the physical quantities are moving in wave propagation.

6 Conclusions

This study solves the mathematical model for studying the influence of rotation and magnetic field in anisotropic piezo-thermoelastic materials for two-dimensional propagation of plane harmonic waves. Recent interest in the piezoelectric materials stems from their potential applications in intelligent structural systems, and piezoelectric is currently enjoying a greatest resurgence in both fundamental research and technical applications. The thermoelasticity is concerned with the study of thermo-dynamics

Fig. 15 (3D) Distribution of temperature T versus the components of distance based on (G–L) model at $\Omega = 0.5$ and $H_0 = 10^8$

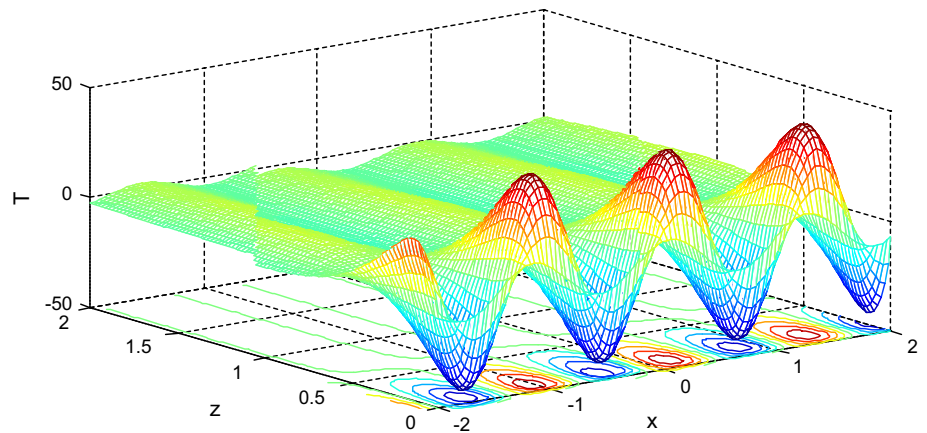


Fig. 16 (3D) Distribution of the stress component σ_{xx} versus the components of distance based on (G–L) model at $\Omega = 0.5$ and $H_0 = 10^8$

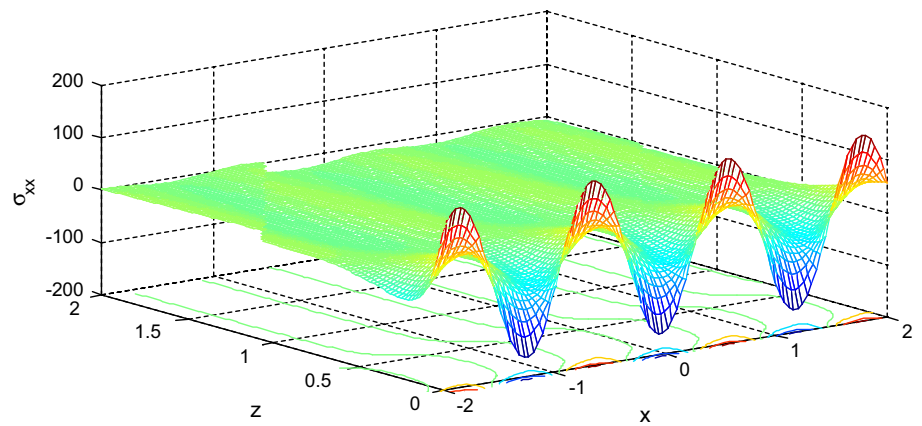
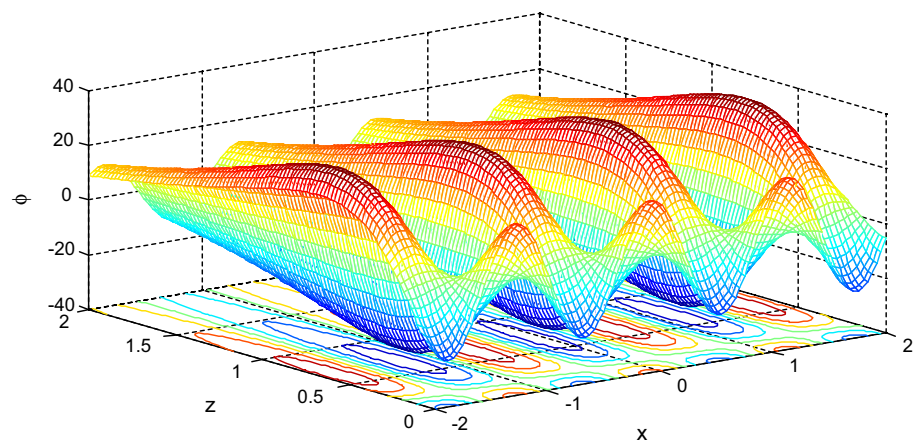


Fig. 17 (3D) Electric potential against both components of distance based on G–L model at $\Omega = 0.5$ and $H_0 = 10^8$

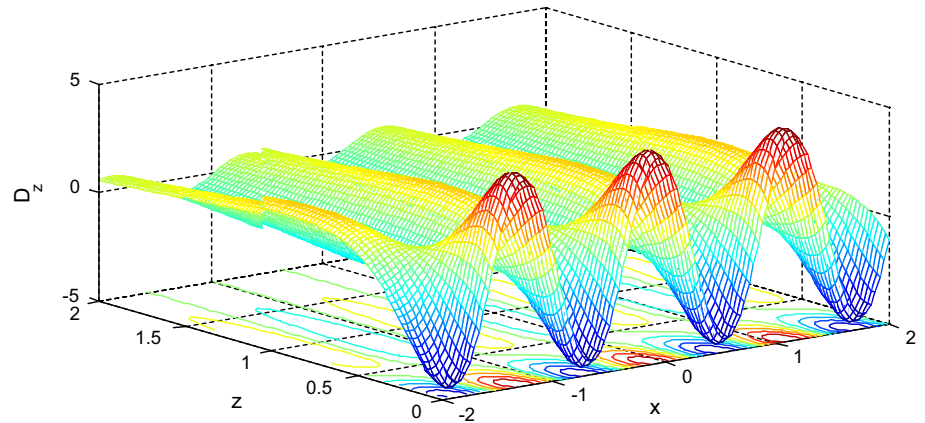


system of bodies in equilibrium, whose interactions with the surroundings are limited to mechanical work, heat exchange and external work. Comparing the figures which obtained under the two theories, important phenomena have observed that,

- Analytical solutions based upon normal mode analysis for thermoelastic problem in solids have been developed and used.

- The method which used in the present article is applicable to a wide range of problems in hydrodynamics and thermoelasticity.
- The value of all physical quantities converges to zero with an increase in distance z and all functions are continuous. All the physical quantities satisfy the boundary conditions.

Fig. 18 (3D) Distribution of electric displacement D_z against both components of distance based on G–L model at $\Omega = 0.5$ and $H_0 = 10^8$



- Deformation of a body depends on the nature of forced applied as well as the type of boundary conditions.
- The comparisons of two theories of thermoelasticity, (CT) and (G–L) theories are carried out.

Appendix A

$$\begin{aligned} \delta_1 &= \frac{C_{11} + \mu_0 H_0^2}{\rho v_p^2}, \quad \delta_2 = \frac{C_{44}}{\rho v_p^2}, \quad \delta_3 = \frac{C_{13} + C_{44} + \mu_0 H_0^2}{\rho v_p^2}, \\ \delta_4 &= \frac{(e_{31} + e_{15})}{e_{33}}, \quad \delta_5 = \left(1 + \frac{\epsilon_0 \mu_0^2 H_0^2}{\rho}\right), \\ \delta_6 &= \frac{C_{33} + \mu_0 H_0^2}{\rho v_p^2}, \quad \delta_7 = \frac{e_{15}}{e_{33}}, \quad \delta_8 = -\frac{\beta_3}{\beta_1}, \\ \delta_9 &= \frac{(e_{15} + e_{31})}{\rho v_p^2}, \quad \delta_{10} = \frac{e_{15}}{\rho v_p^2}, \quad \delta_{11} = \frac{e_{33}}{\rho v_p^2}, \\ \delta_{12} &= -\frac{\epsilon_{11}}{e_{33}}, \quad \delta_{13} = -\frac{\epsilon_{33}}{e_{33}}, \quad \delta_{14} = \frac{p_3}{\beta_1}, \quad \delta_{15} = \frac{K_1 \omega^*}{\rho C_e v_p^2}, \\ \delta_{16} &= \frac{K_3 \omega^*}{\rho C_e v_p^2}, \quad \delta_{17} = \frac{\beta_1^2 T_0}{\rho^2 C_e v_p^2}, \\ \delta_{18} &= \frac{\beta_1 \beta_3 T_0}{\rho^2 C_e v_p^2}, \quad \delta_{19} = -\frac{p_3 \beta_1 T_0}{\rho C_e e_{33}}. \end{aligned} \quad (52)$$

$$\begin{aligned} A_1 &= -\frac{(a^2 \delta_1 - a^2 c^2 \delta_5 - \Omega^2)}{\delta_2}, \quad A_2 = \frac{ia \delta_3}{\delta_2}, \\ A_3 &= \frac{2iac \Omega}{\delta_2}, \quad A_4 = \frac{ia \delta_4}{\delta_2}, \quad A_5 = -\frac{ia(1 - iact_1)}{\delta_2}, \\ A_6 &= \frac{ia \delta_3}{\delta_6}, \quad A_7 = -\frac{2iac \Omega}{\delta_6}, \end{aligned}$$

$$\begin{aligned} A_8 &= -\frac{(a^2 \delta_2 - a^2 c^2 \delta_5 - \Omega^2)}{\delta_6}, \quad A_9 = \frac{1}{\delta_6}, \\ A_{10} &= -\frac{a^2 \delta_7}{\delta_6}, \quad A_{11} = \frac{\delta_8(1 - iact_1)}{\delta_6}, \quad A_{12} = \frac{ia \delta_9}{\delta_{11}}, \\ A_{13} &= -\frac{a^2 \delta_{10}}{\delta_{11}}, \quad A_{14} = \frac{\delta_{13}}{\delta_{11}}, \\ A_{15} &= -\frac{a^2 \delta_{12}}{\delta_{11}}, \quad A_{16} = \frac{\delta_{14}(1 - iact_1)}{\delta_{11}}, \\ A_{17} &= -\frac{a^2 c \delta_{17}}{\delta_{16}}, \quad A_{18} = \frac{iac \delta_{18}}{\delta_{16}}, \quad A_{19} = \frac{iac \delta_{19}}{\delta_{16}}, \\ A_{20} &= -\frac{(a^2 \delta_{15} - iac - a^2 c^2 t_0)}{\delta_{16}}. \end{aligned} \quad (53)$$

$$\begin{aligned} A &= -\left(\frac{1}{A_{14} - A_9}\right) (A_{14} A_{20} + A_{15} - A_{16} A_{19} + A_8 A_{14} \\ &\quad - A_9 A_{13} - A_9 A_{20} + A_9 A_{16} A_{18} - A_{10} \\ &\quad + A_{11} A_{19} - A_{11} A_{14} A_{18} + A_1 A_{14} - A_1 A_9 - A_2 A_6 A_{14} \\ &\quad + A_2 A_9 A_{12} + A_4 A_6 - A_4 A_{12}) \end{aligned} \quad (54)$$

$$\begin{aligned} B &= \left(\frac{1}{A_{14} - A_9}\right) (A_{15} A_{20} + A_8 A_{14} A_{20} + A_8 A_{15} - A_8 A_{16} A_{19} \\ &\quad - A_9 A_{13} A_{20} - A_{10} A_{13} - A_{10} A_{20} \\ &\quad + A_{10} A_{16} A_{18} + A_{11} A_{13} A_{19} - A_{11} A_{15} A_{18} + A_1 A_{14} A_{20} \\ &\quad + A_1 A_{15} - A_1 A_{16} A_{19} + A_1 A_8 A_{14} \\ &\quad - A_1 A_9 A_{13} - A_1 A_9 A_{20} + A_1 A_9 A_{16} A_{18} - A_1 A_{10} \\ &\quad + A_1 A_{11} A_{19} - A_1 A_{11} A_{14} A_{18} - A_2 A_6 A_{14} A_{20} \\ &\quad - A_2 A_6 A_{15} + A_2 A_6 A_{16} A_{19} + A_2 A_9 A_{12} A_{20} \\ &\quad - A_2 A_9 A_{16} A_{17} + A_2 A_{10} A_{12} - A_2 A_{11} A_{12} A_{19} \\ &\quad + A_2 A_{11} A_{14} A_{17} - A_3 A_7 A_{14} + A_4 A_6 A_{13} + A_4 A_6 A_{20}) \end{aligned}$$

$$\begin{aligned}
 & -A_4A_6A_{16}A_{18} - A_4A_{12}A_{20} + A_4A_{16}A_{17} \\
 & -A_4A_8A_{12} + A_4A_{11}A_{12}A_{18} - A_4A_{11}A_{17} - A_5A_6A_{19} \\
 & + A_5A_6A_{14}A_{18} + A_5A_{12}A_{19} \\
 & - A_5A_{14}A_{17} - A_5A_9A_{12}A_{18} + A_5A_9A_{17}). \tag{55}
 \end{aligned}$$

$$\begin{aligned}
 C = & -\left(\frac{1}{A_{14} - A_9}\right)(A_8A_{15}A_{20} - A_{10}A_{13}A_{20} + A_1A_{15}A_{20} \\
 & + A_1A_8A_{14}A_{20} + A_1A_8A_{15} - A_1A_8A_{16}A_{19} \\
 & - A_1A_9A_{13}A_{20} - A_1A_{10}A_{13} - A_1A_{10}A_{20} \\
 & + A_1A_{10}A_{16}A_{18} + A_1A_{11}A_{13}A_{19} - A_1A_{11}A_{15}A_{18} \\
 & - A_2A_6A_{15}A_{20} + A_2A_{10}A_{12}A_{20} - A_2A_{10}A_{16}A_{17} \\
 & + A_2A_{11}A_{15}A_{17} - A_3A_7A_{14}A_{20} - A_3A_7A_{15} \\
 & + A_3A_7A_{16}A_{19} + A_4A_6A_{13}A_{20} - A_4A_8A_{12}A_{20} \\
 & + A_4A_8A_{16}A_{17} - A_4A_{11}A_{13}A_{17} - A_5A_6A_{13}A_{19} \\
 & + A_5A_6A_{15}A_{18} - A_5A_{15}A_{17} + A_5A_8A_{12}A_{19} \\
 & - A_5A_8A_{14}A_{17} + A_5A_9A_{13}A_{17} - A_5A_{10}A_{12}A_{18} \\
 & + A_5A_{10}A_{17}). \tag{56}
 \end{aligned}$$

$$\begin{aligned}
 E = & \left(\frac{1}{A_{14} - A_9}\right)(A_1A_8A_{15}A_{20} - A_1A_{10}A_{13}A_{20} \\
 & - A_3A_7A_{15}A_{20} - A_5A_8A_{15}A_{17} + A_5A_{10}A_{13}A_{17}). \tag{57}
 \end{aligned}$$

Appendix B

$$\begin{aligned}
 H_{1n} = & -\frac{s_{1n}}{s_{2n}}, \quad H_{2n} = -\frac{(q_{1n} + q_{2n}H_{1n})}{q_{3n}}, \\
 H_{3n} = & -\frac{1}{A_5}[(k_n^2 + A_1) + (-A_2k_n + A_3)H_{1n} \\
 & - A_4k_nH_{2n}], \\
 H_{4n} = & r_1 - l_2k_nH_{1n} - l_3k_nH_{2n} + r_2H_{3n}, \\
 H_{5n} = & r_3 - l_4k_nH_{1n} - k_nH_{2n} + r_4H_{3n}, \\
 H_{6n} = & -\delta_2k_n + r_5H_{1n} + r_6H_{2n}, \\
 H_{7n} = & -l_5k_n + r_7H_{1n} + r_8H_{2n}, \\
 H_{8n} = & r_9 - l_{12}k_nH_{1n} - l_9k_nH_{2n} + r_{10}H_{3n}, \quad n = 1, 2, 3, 4. \tag{58}
 \end{aligned}$$

$$\begin{aligned}
 q_{1n} = & A_{11}k_n^3 + (A_1A_{11} - A_5A_6)k_n + A_5A_7, \\
 q_{2n} = & (-A_2A_{11} + A_5)k_n^2 + A_3A_{11}k_n + A_5A_8, \\
 q_{3n} = & (-A_4A_{11} + A_5A_9)k_n^2 + A_5A_{10}, \\
 q_{4n} = & A_{16}k_n^3 + (A_1A_{16} - A_5A_{12})k_n,
 \end{aligned}$$

$$\begin{aligned}
 q_{5n} = & (A_5 - A_2A_{16})k_n^2 + A_3A_{16}k_n + A_5A_{13}, \\
 q_{6n} = & (A_5A_{14} - A_4A_{16})k_n^2 + A_5A_{15}, \tag{59}
 \end{aligned}$$

$$s_{1n} = q_{1n}q_{6n} - q_{3n}q_{4n}, \quad s_{2n} = q_{2n}q_{6n} - q_{3n}q_{5n}, \tag{60}$$

$$\begin{aligned}
 l_1 = & \frac{C_{11}}{\rho v_p^2}, \quad l_2 = \frac{C_{13}}{\rho v_p^2}, \quad l_3 = \frac{e_{31}}{e_{33}}, \\
 l_4 = & \frac{C_{33}}{\rho v_p^2}, \quad l_5 = \frac{e_{15}\beta_1 T_0}{e\rho v_p^2}, \quad l_6 = -\frac{\epsilon_{11}\beta_1 T_0}{e_{33}e}, \\
 l_7 = & \frac{e_{31}\beta_1 T_0}{e\rho v_p^2}, \quad l_8 = \frac{e_{33}\beta_1 T_0}{e\rho v_p^2}, \quad l_9 = -\frac{\epsilon_{33}\beta_1 T_0}{e_{33}e}, \\
 l_{10} = & \frac{P_3 T_0}{e}, \tag{61}
 \end{aligned}$$

$$\begin{aligned}
 \{r_1, r_3, r_5, r_6, r_7, r_8, r_9\} = & ia\{l_1, l_2, \delta_2, \delta_7, l_5, l_6, l_7\}, \\
 r_2 = & -(1 - ia ct_1), \quad r_4 = \delta_8(1 - ia ct_1), \\
 r_{10} = & l_{10}(1 - ia ct_1). \tag{62}
 \end{aligned}$$

References

Ashida F, Tauchert TR, Noda N (1994) A general solution technique for piezothermoelasticity of hexagonal solids of class 6 mm in Cartesian coordinates. *ZAMM* 74(2):87–95

Chandrasekharaiah DS (1984) A temperature rate dependent theory of piezo-electricity. *J Therm Stress* 7:293–306

Chandrasekharaiah DS (1988) A generalized linear thermoelasticity theory of piezoelectric media. *Acta Mech* 71:39–49

Curie J, Curie P (1880) Development par compression de l’etricite polaire das les cristaus hemledres a face inclines. *C R Acad Sci* 91:294–295

El-Naggar AM, Abd-Alla AM (1989) Rayleigh waves in magneto-thermoelastic half-space under initial stress. *J Earth Moon Planets* 45:175–185

He TH, Tian XG, Yapeng S (2002a) Two dimensional generalized thermal shock problems of a thick piezoelectric plate of infinite extent. *Int J Eng Sci* 40:2249–2264

He TH, Tian XG, Yapeng S (2002b) State space approach to one-dimensional thermal shock problem for a semi-infinite piezoelectric rod. *Int J Eng Sci* 40:1081–1097

Mindlin RD (1961) On the equations of motion of piezoelectric crystals, in problems of continuum mechanics. *SIAM, Philadelphia*. N I Muskhelishvili ‘s Birthday 70:282–290

Nowachi W (1978) Some general theorems of thermo-piezoelectricity. *J Thermal Stresses* 1:171–182

Nowachi W (1983) Mathematical models of phenomenological piezoelectricity. *New Problems in Mechanics of Continua*. University of Waterloo Press, Waterloo, pp 29–49

Othman MIA (2002) Lord-Shulman theory under the dependence of the modulus of elasticity on the reference temperature in two-dimensional generalized thermoelasticity. *J Therm Stress* 25:1027–1045

Othman MIA (2005) Generalized electromagnetic-thermoelastic plane waves by thermal shock problems in a finite conductivity half-space with one relaxation time. *Multi Model Mater Struct* 1:231–250

Othman MIA, Abbas IA (2014) Effect of rotation on plane waves in generalized thermo-microstretch elastic solid comparison of different theories using finite element method. *Can J Phys* 92:1269–1277

Othman MIA, Abbas IA (2015) Effect of rotation on a magneto-thermoelastic hollow cylinder with energy dissipation using finite element method. *J Comp Theor Nanosci* 12:2399–2404

- Othman MIA, Ahmed EAA (2016) Influence of the gravitational field on piezo-thermoelastic rotating medium with G–L theory. *Eur Phys J Plus* 131:358–369
- Othman MIA, Elmaklizi JD (2013) 2-D problem of generalized magneto-thermoelastic diffusion with temperature dependent elastic moduli. *J Phys* 2:4–11
- Othman MIA, Kumar R (2009) Reflection of magneto-thermoelastic wave under temperature dependent properties in generalized thermoelasticity with four theories. *Int Commun Heat Mass Transfer* 36:513–520
- Othman MIA, Hasona WM, Eraki EEM (2013) Influence of gravity field and rotation on a generalized thermoelastic medium using a dual-phase-lag model. *J Thermoelast* 1:12–22
- Othman MIA, Hasona WM, Abd-Elaziz EM (2014) Effect of rotation on micro-polar generalized thermoelasticity with two-temperature using a dual-phase-lag model. *Can J Phys* 92:148–159
- Qin QH, Yang QS (2008) *Macro-micro theory on multi field coupling behavior of heterogeneous materials*. Springer, Berlin, Heidelberg, New York
- Said SM (2016) Influence of gravity on generalized magneto-thermoelastic medium for three-phase-lag. *J Comp Appl Math* 291:142–157
- Schoenberg M, Censor D (1973) Elastic waves in rotating media. *Quart Appl Maths* 31:115–125
- Sharma JN, Kumar M (2000) Plane harmonic waves in piezo-thermoelastic materials. *Indian J Eng Mater Sci* 7:434–442
- Sharma JN, Pal M, Chand D (2005) Propagation characteristics of Rayleigh waves in transversely isotropic piezothermoelastic materials. *J Sound Vib* 284:227–248
- Tichy J, Erhart J, Kittinger E, Privratska J (2010) *Fundamentals of piezoelectric Sensorics*. Springer, Berlin, Heidelberg, New York
- Youssef HM, Bassiouny E (2008) Two-temperature generalized thermo-piezo-elasticity for one dimensional problem state space approach. *Comp Methods Sci Tech* 14:55–64